Transactions of the VŠB – Technical University of Ostrava, Mechanical Series
No. 1, 2010, vol. LVI
article No. 1775

Lukáš ZAVADIL[*], Sylva DRÁBKOVÁ [**]

DETERMINATION OF RADIAL FORCE IN HYDRODYNAMIC PUMP USING NUMERICAL MODELLING

STANOVENÍ RADIÁLNÍ SÍLY V HYDRODYNAMICKÉM ČERPADLE S VYUŽITÍM NUMERICKÉHO MODELOVÁNÍ

Abstract

This paper deals with determination of radial force for a centrifugal pump impeller using the numerical modelling as a tool. Fluent software package was applied to investigate the flow in a centrifugal pump with given parameters Qv = 0.007 m^3s^{-1}, H = 80 m, n = 2 900 min^{-1} designed at the Victor Kaplan Department of Fluid Engineering, Energy Institute, Technical university Brno. The incompressible, unsteady flow (and steady to compare) was modelled in 3D geometry consisting of inlet part, impeller and volute. Results obtained by numerical modelling were compared with predictions of radial force using empirical formulas defined by several authors.

Abstrakt

Článek se zabývá určením radiální síly při práci odstředivého čerpadla pomocí numerického modelování. Předmětem numerického experimentu je modelování proudění v pracovních prostorách čerpadla s parametry Qv = 0.007 m^3s^{-1}, H = 80 m, n = 2 900 min^{-1}. Geometrie výpočtové oblasti je definována dle výkresové dokumentace poskytnuté Odborem fluidního inženýrství Viktora Kaplana, VUT Brno a zahrnuje vstupní část, oběžné kolo a spirálu odstředivého čerpadla. Byly realizovány výpočty pro ustálené proudění i časově závislou úlohu. Výsledky numerického modelování jsou následně porovnány s hodnotami radiální síly určené pomocí empirických vztahů dle řady autorů.

1 INTRODUCTION

The radial load on the impeller is caused by non-uniform pressure distribution around the impeller periphery in centrifugal pump. As a result shaft deflection appears. The consequences of severe shaft deflection include high wear rate on bearings, shaft seal leakage, and fatigue bending of the pump shaft. Dynamic character of the radial force can also excite vibrations which can lead to the pump failure. The value of radial force is minimal in the best efficiency point (BEP) but grows with both lower and higher flow rate. In general, shaft deflection is most problematic when a pump is operated at low flow conditions. Dynamic character of the radial force may excite in vibrations, which can cause a pump failure, especially at double suction pumps, because there are the bearings mounted far away from each other. Pump shafts must be designed to sustain the load and that is why determination of radial force is of great importance. We can use empirical formulas for that purpose, but there can be another way, assignment of the radial force using numerical modelling of the flow through impeller and volute.

Design of the volute can affect the behavior and magnitude of radial force. For example double volute (see Fig. 1) has constant value of the radial force over the range of capacity, but usually the efficiency decreases. Fig. 1 shows relation between radial force and capacity for commonly used types of the volute casing.

[*] Ing., VŠB-Technical University of Ostrava, Faculty of Mechanical Engineering, Department of Hydromechanic and Hydraulic Equipment, 17. listopadu 15/2172, 708 33 Ostrava-Poruba, Czech Republic, tel.: (+420) 59 732 5753, e-mail: lukas.zavadil.st1@vsb.cz

[**] doc., Ing., Ph.D., VŠB-Technical University of Ostrava, Faculty of Mechanical Engineering, Department of Hydromechanic and Hydraulic Equipment, 17. listopadu 15/2172, 708 33 Ostrava-Poruba, Czech Republic, tel.: (+420) 59 732 4386, e-mail: sylva.drabkova@vsb.cz

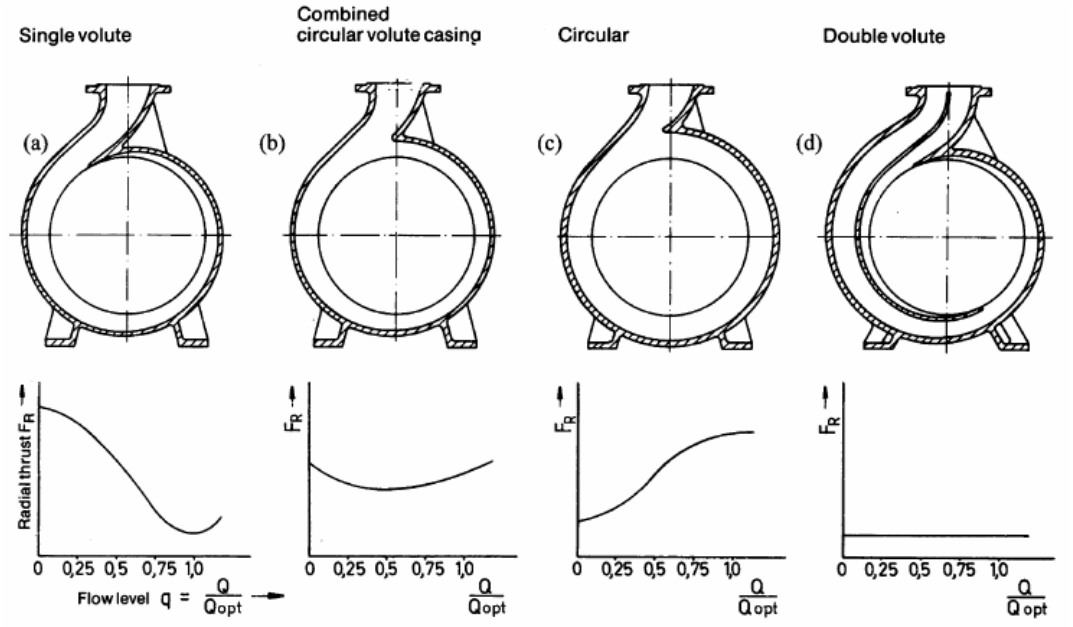

Fig. 1 The shape of the volute casing and radial thrust [9]

2 NUMERICAL SIMULATION

Numerical modelling was applied to investigate the flow in a single-stage centrifugal pump with horizontally mounted shaft. Geometry of the computational domain includes inlet part, impeller and single volute, see Fig. 2. This approach allows simulate interaction between impeller and volute. Design parameters of the pump were n = 2900 min^{-1}, H = 80 m, Q_V = 0.007 m^{3}s^{-1}. This pump provides high head and low flow which yields a low value of non-dimensional specific speed:

$$n_b = n \cdot \frac{\sqrt{Q_v}}{Y^{0,75}} = 0{,}02727 \tag{1}$$

where:

n – rotational speed [s^{-1}],

Q_V – flow rate [m^3·s^{-1}],

Y – specific energy [J·kg^{-1}].

FLUENT release 6.3.26 was applied for numerical modelling of flow through a pump. The incompressible, unsteady (and steady to compare) flow was modeled in complex 3D geometry. The problem involves multiple moving parts as well as stationary surfaces. In Fluent, two approaches can be applied for the modeling of such cases:

- Multiple Rotating Reference Frames
  - *Multiple Reference Frame model (*MRF*)*
  - *Mixing Plane Model (*MPM*)*
- Sliding Mesh Model (SMM)

Both the MRF and MPM approaches are steady-state approximations, and differ primarily in the manner in which conditions at the interfaces are treated. In this case results are given for one position of blades of the impeller against volute. Simulations in this case take less of a time but this approach neglect dynamic effects of flow. The "*Sliding mesh*" model (SMM approach) is unsteady

due to the motion of the mesh with time. This approach was applied in most cases. Data sampling for time statistics was applied which enable to compute the time average (mean) of the instantaneous values and root-mean-squares of the fluctuating values sampled during the calculation. The time step was constant during simulation with value Δt = 0.001s. Turbulent model k-ω SST was used for the simulations. Non-conformal grid was generated with 1688662 cells. Boundary layers were attached to blades, wall of volute and to interface between impeller and volute. The detail of the computational grid is shown on Fig. 3.

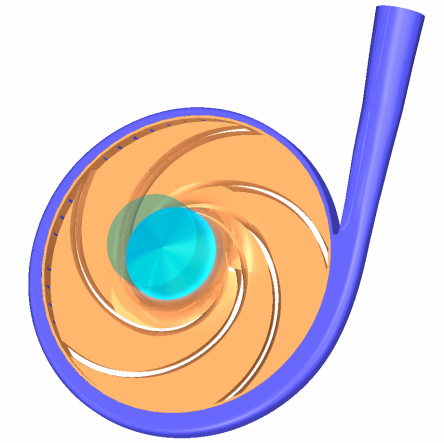

Fig. 2 Schematic of the modeled geometry

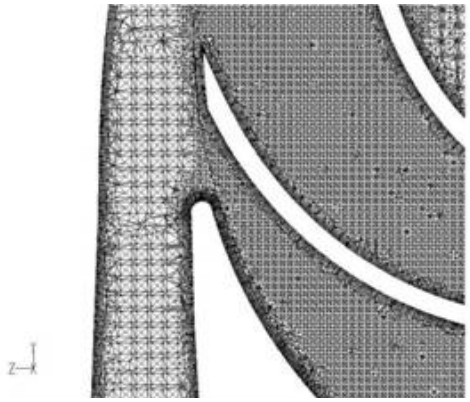

Fig. 3 Detail of the computational grid

3 RESULTS

The total force component along the specified force vector on a wall zone is computed by summing the dot product of the pressure and viscous forces on each face with the specified force vector.

$$\underbrace{F_a}_{\text{total force component}} = \underbrace{\vec{a}\cdot\vec{F_p}}_{\text{pressure force component}} + \underbrace{\vec{a}\cdot\vec{F_v}}_{\text{viscous force component}} \tag{2}$$

The terms in this summation represent the pressure and viscous force components in the direction of the vector $\vec{a}$. In addition to the actual pressure, viscous, and total forces, the associated force coefficients are also computed. Lift coefficient was used for assignment of radial force which acts on the impeller:

$$F = C_L \cdot \frac{1}{2} \cdot \rho \cdot S \cdot v^2 \cdot \Rightarrow C_L = \frac{2 \cdot F}{\rho S v^2} \tag{3}$$

where:

C_L – lift coefficient [-],

ρ – reference density [kg·m^{-3}],

S – reference area [m^2],

v – reference velocity [m·s^{-1}].

Lift coefficient C_L was recorded in each time step using the option Solve/Monitors/Force. Radial hydraulic load acts on an impeller at right angles to the shaft, so lift coefficients on Y and Z axis were monitored. Resultant force was calculated from the components and the direction of the force vector was defined for various values of capacity.

The same procedure is described in [5]. Fig. 4 shows lift coefficient recorded on Y axis. Time variation of the coefficient can be observed because of inherent flow unsteadiness and blade passing forces. The casting impeller usually is not perfectly symmetric and the vanes are not identical. That is why the dynamic component of radial force occurs. For the design of bearings and shafting, it is usually sufficient to know the time-averaged value of radial force F, and in the pump literature this force is then called the static component of the radial force.

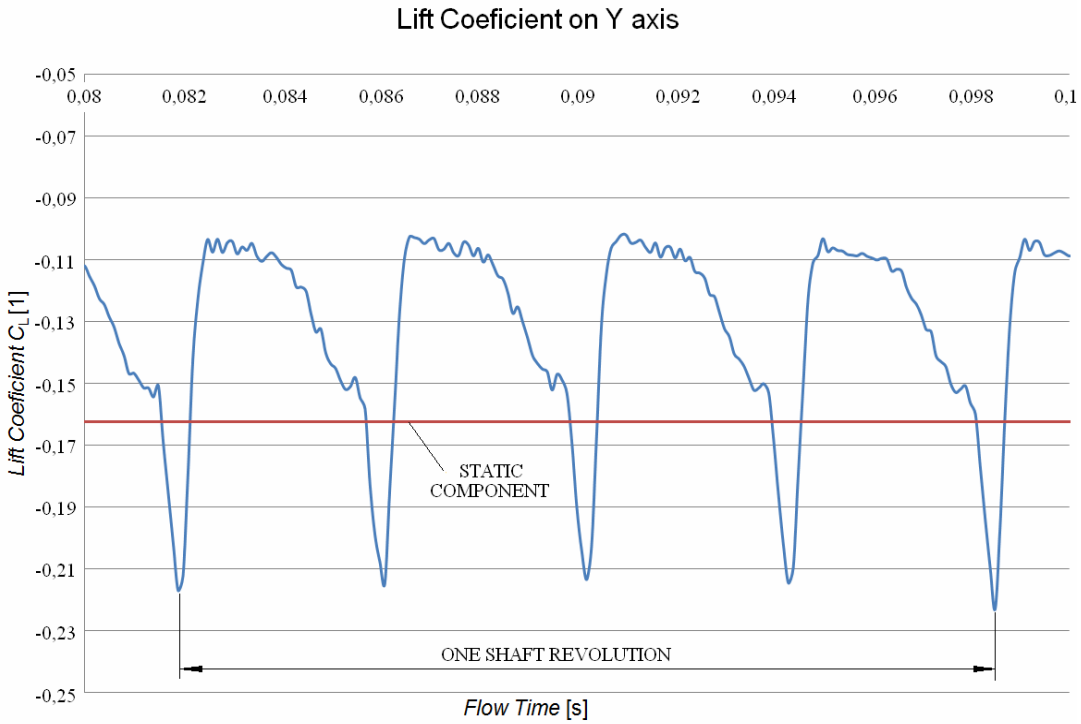

Fig. 4 The record of vertical component of the radial force

Fig. 5 shows the value of the radial force and its direction in dependence on capacity obtained by numerical modeling. Reference axes show value of the radial force in Y and Z directions; from these values the total radial force can be calculated. Values at points indicate percentage of optimal capacity. The direction of radial force can be obtained by connecting the coordinate basic origin with the point of given flow rate. We can see that the radial force changes its direction, for the flow rate $Q < Q_n$ the radial force is oriented to the 1st quadrant and for flow rates $Q > Q_n$ it changes its direction to the 4th quadrant.

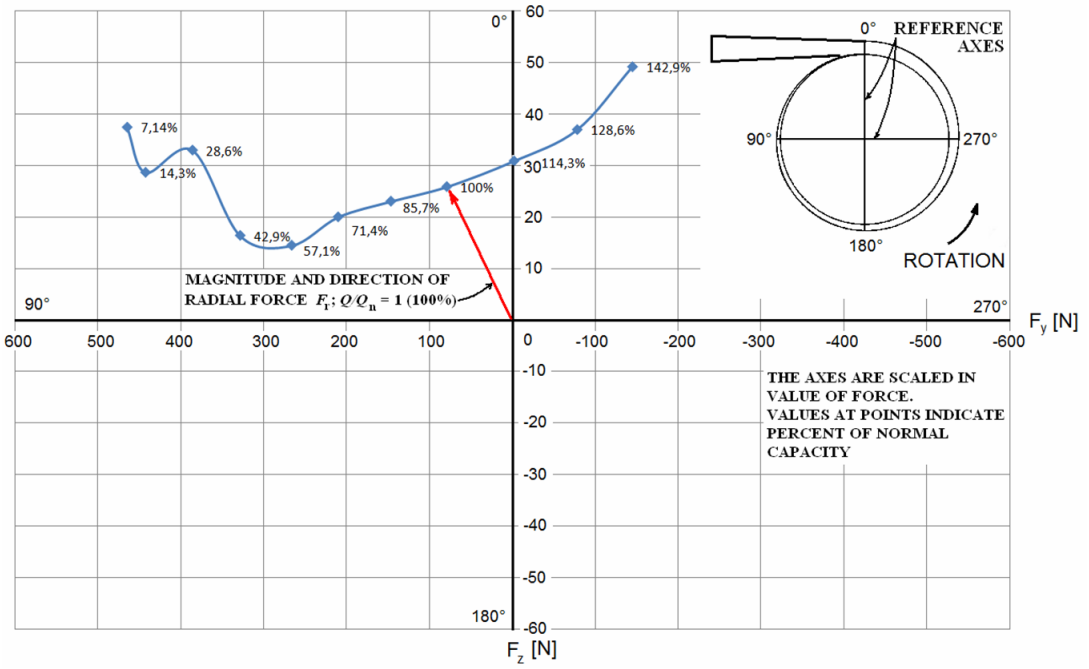

Fig. 5 Diagram of the radial force determined by numerical modelling

4 COMPARISON WITH EMPIRICAL FORMULAS

Works dealing with the existence of the radial force and attempts to determine it date back to the 30s of the 20th century. Many contributions to this problem were published in 1960s and 1970s especially by Agostinelli (1960), Iverson (1960), Biheller (1965), Grabow (1964), Chamieh (1985), Stepanoff (1957). Because of the absence of experimental data for verification of calculated radial force, the approximate radial force was calculated using the empirical formulas according to Stepanoff, Agostinelli, Mackay, Biheller, KSB company. Stepanoff proposed a simple empirical model based on impeller geometry, pump head and capacity to estimate the radial resultant forces. Agostinelli et al. extended Stepanoff's model taking to account the effect of specific speed on radial forces. Biheller developed an equation to predict static radial pump forces applicable for a wide range of pump types and operating conditions. The obtained results can differ according to applied formulae.

Empirical formulas shown below were used for comparison with values obtained by numerical modelling. Equations and diagrams for assignment of constants can be found in literature, but in some cases different values of constants are presented, for example in Biheller´s equation.

- Stepanoff [1]

$$F_0 = K \cdot H \cdot d_2 \cdot b_2' \tag{4}$$

$$K = 0.36 \cdot \left[1 - \left(\frac{Q}{Q_n} \right)^2 \right] \tag{5}$$

where: H – head (m), d_2 – impeller diameter (m), b_2 – impeller width including shrouds (m). K– radial thrust factor, F_0 – radial force (kg).

❑ Agostinelli [3]

$$F_r = k \cdot K_r \cdot (sp.gr.) \cdot H \cdot D_2 \cdot b_2 \tag{6}$$

where:
sp.gr – specific gravity of the pumped liquid (equal to unity for cold water), k – 9790, Kr – experimentally determined coefficient, H – pump head (m), b_2 – impeller width at discharge including shrouds (m), D_2 – outlet diameter of impeller (m), F_r – radial thrust (N).

❑ Mackay [4]

$$F_{so} = K_{SO} \cdot P_{SO} \cdot D \cdot B \tag{7}$$

$$F = F_{SO} \cdot \left[1 - \left(\frac{Q}{Q_n} \right)^x \right] \tag{8}$$

where:

K_{SO} – radial thrust factor that can be established from the impeller design and tends to vary between 0.15 and 0.38 depending on the design and its specific speed, P_{SO} – differential pressure at shutoff (psi), D – impeller diameter (in), B – impeller width at perimeter including shrouds (in), x – exponent, may be assumed to vary linearly between 0.7 at an impeller specific speed 500, and a value of 3.3 at an impeller specific speed of 3500, F – radial force (pounds).

- **Biheller** [1]

$$F = 0.1511 \cdot u_2^2 \cdot A_j \cdot \rho \cdot 10^{-(1,13\Delta A/A)} \cdot \sqrt{1 - \left(\frac{Q}{Q_n} \right)^2 - 2\left(\frac{Q}{Q_n} \right) \cos\left\{ \frac{\pi}{2} \left(\frac{Q}{Q_n} - 1 \right) \right\}} \tag{9}$$

where:

ρ – specific mass (kgsec^2/m^4) , A_j – total impeller project area (m^2), F – radial force (kg).

- **KSB pumps** [2]

$$F_R = \kappa \cdot \rho \cdot g \cdot H \cdot D_2 \cdot b_2 \tag{10}$$

where:

κ – radial thrust factor, ρ – density of the pumped liquid (kg/m^3), g – gravity (m/s^2),
H – head (m), D_2 – impeller diameter (m), b_2 – impeller width (m), F_R – radial force (N).

Fig. 6 shows comparison of results obtained by numerical modeling and from empirical formulas. It can be seen that results obtained by empirical formulas from equations (4) to (10) are different. This can be affected by parameters of the modeled pump. Modeled pump has a low value of flow rate but a high value of head, this leads to a low value of specific speed. Especially formulas given by Agostinelli (6) and KSB (10) are depending on specific speed, this can be a reason why they give different values, in general these formulas are recommended for higher values of specific speed.

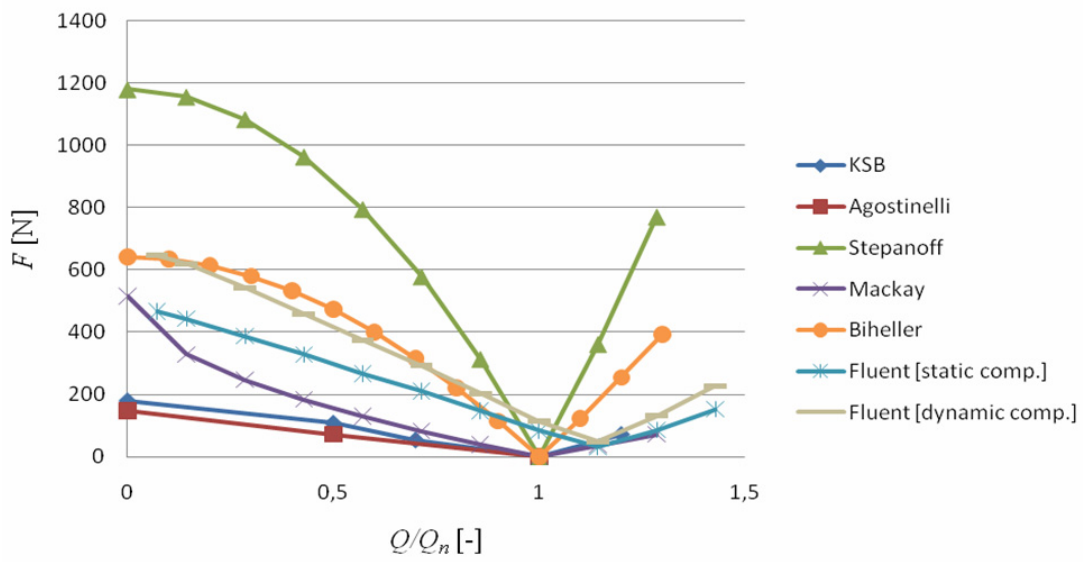

Fig. 6 Comparison of results obtained by numerical modeling with results obtained from empirical formulas

5 CONCLUSION

Empirical formulas are useful for determination of static component of the radial force. The value of dynamic load is higher and this fact must be accepted during the design of impeller shaft. Experimental and numerical approaches contributed to the understanding of the highly complex flow interactions that occur in a centrifugal pump. Results from numerical modelling show the oscillation of the radial force and enable to determine the mean load, magnitude and direction of radial force.

Results of numerical modeling were compared with values obtained from empirical formulas. The results are close to those predicted by Biheller (9) and Mackay (7, 8). Stepanoff´s equation gives higher values than others, but this can contribute to the safety of the shaft design. The most adequate is Biheller´s equation for calculation of static component of the radial force. It can be further multiplied by the safety constant k = 1.2 – 1.4 to account for dynamic effects.

Radial force is expected to reach its minimum in BEP. This was not confirmed by numerical modelling, as minimal value of the radial force was predicted behind BEP. Further numerical experiments are required to increase the accuracy of radial force prediction. There are others questions which can be tested, for example influence of computational grid and applied turbulence model.

6 REFERENCES

[1] [1] UCHIDA, N., IMAICHI, K., SHIRAI, T. *Radial Force on the Impeller of a Centrifugal Pump**. [online], Datum poslední revize 6.1.2010. Dostupné z < http://nels.nii.ac.jp/els/110002360509.pdf?id =ART0002639135&type=pdf&lang=en&host=cinii&order_no=&ppv_ttyp=0&lang_sw=&no =1262706270&cp= >.

[2] *Projektování čerpadel*. KSB pumpy & armatury s.r.o., 48s.

[3] KARASSIK, I. J., MESSINA, J. P., COOPER, P., HEALD, CH. C. *Pump handbook third edition*. [online], Datum poslední revize 1.5.2010. Dostupné z < http://books.google.cz/books?id =yU5TyJrOMF8C&printsec=frontcover&source=gbs_navlinav_s#v=onepage&q=&f=false >, s. 373-375.

[4] MACKAY, R. *Shaft Deflection Part One: The Cause*. [online], Datum poslední revize 3.11.2004. Dostupné z < http://www.pump-zone.com/articles/22.pdf >.

[5] BLÁHA, J., BRADA, K. Příručka čerpací techniky. 1. vyd. Praha: ČVUT, 1997. 289 s. ISBN 80-01-01626-9.

[6] ZAVADIL, L. *Numerické modelování proudění v hydrodynamickém čerpadle*. Ostrava, 2009. Diplomová práce, Fakulta strojní, VŠB-TU Ostrava

[7] FLUENT 6.3.26 – *User´s guide*. Fluent Inc. 2003 [online]. Datum poslední revize 3.10.2006 [cit. 2008-12-08]. Dostupné z < http://spc.vsb.cz/portal/cz/documentation/manual/doc.vsb.cz/Aplikacni%20software/FlueFl_6.3.26/pdf/ug/flug.pdf >.

[8] BRENNEN, C. E. *Hydrodynamics of Pumps*. [online] Datum poslední revise 16.6.2004. Dostupné z < http://caltechbook.library.caltech.edu/22/3/pumbook.pdf >.

[9] *Centrifugal pump design*. Technical appendix, KSB, Frankenthal, Germany.